

A new profile for the worm gear drive of a spiral gear

S Totolici¹, V G Teodor², N Baroiu² and N Oancea²

¹”Dunărea de Jos” University of Galati, Faculty of Economics and Business Administration, Department of Business Administration;

²”Dunărea de Jos” University of Galați, Faculty of Mechanical Engineering, Department of Manufacturing Engineering

E-mail: virgil.teodor@ugal.ro

Abstract. The worm-spiral wheel frontal gear, known as the Helicon gear is a constructive variant of the worm gearing. The advantage of this construction is the reduced overall size in the plane of the spiral wheel, if compared with the usual worm gearing. This paper presents the geometrical modeling of this gearing type in order to define its constructive elements. It is accepted that in the proposed modeling the worm is an Archimede’s worm, due to technological considerations. It also studies the constructive variant of the worm gear which ensures a longer contact line, with influences on the reduction of the gear loading. It also presents the constructive form of the new hob mill for the milling of the in-plane wheel of the spiral gear. Experimental measurements are presented for the input and output torque of a reducer with spiral gear, with a circular axial profile worm.

1. Introduction

The worm-spiral wheel frontal gear represents a constructive variant of worm gearing. These gearing types present the advantage of a reduced overall size regarding the normal worm gearing.

The spiral gears have the transmission ratio in the same domain as the processional gears, Frumușanu et al. [3] but are characterized by decreased torque regarding the processional gears.

However, due to technological difficulties, this gearing type is not very used, especially for large modulus.

Staniek [7] presented the profiling of the in plane wheel of the spiral gear, based on the general theory of the surface enveloping, knowing the form of the worm mill generating profile. This is done starting from the analytical equations of the tool’s surfaces and the relative velocity between the generated flank and the tool.

Also, Litvin et al. [4] solved the issue regarding the optimization of the spiral gear, from the point of view of the worm misalignment with the centre of the in plane wheel. The solution was determined using computerized simulation of meshing and contact for unloaded and loaded gear drives.

Concerning on similarly issues, Riliang Liu et al [7] presented an original approach, for manufacturing complex parts, based on STEP compliant NC programming.

Also, they are known the world achievements, which have devoted these gear types (spiroid and helicon are trademarks of Illinois Tool Work, Chicago), as well as, the recently successes in the East European zone according to Boloș et al. [1]. In the same time, Boloș V. [2] made an extended report of the state of arts regarding the calculus, design and machining technology for this gear’s types.

The present paper presents the geometrical modelling of the worm spiral wheel frontal gear, in order to define some of the constructive elements of this gearing type.



In the following, a new constructive form of the spiroid worm is proposed, versus the known solution of the Archimedes's worm. This new solution will lead to a larger length of the in contact flanks, in order to increase the gear's bearing.

In order to determine the in plane wheel's flank form, the gearing surface and the contact lines, analytical and numerical modelling of the gear's proposed form was made. The study of the spiral gear, at the most of the authors, is based on the analytical method of surfaces enveloping fundamentals, as is described by Litvin et al. [4] and also by Radzevich [6].

The new form of the generating worm, with curved flanks, modelled in this paper, was made, as so as, the milling tool for the generation of the in plane wheel of the gear. A reducer based on the new gear was made, the performance of which was tested from the efficiency of the new transmission.

2. Generation kinematics – reference systems

The worm spiral gear, with wheel teeth of constant height, and the in plane wheel, has the kinematics as defined in figure 1. Here the reference systems for the spiral gear's elements are defined: the worm spiral and the in plane wheel.

Where: xyz is the global reference system, with z axis overlapped to the rotation axis of the in plane wheel; $x_0y_0z_0$ – global reference system, with z_0 axis overlapped to the worm spiral axis; $X_1Y_1Z_1$ – mobile reference system joined with the primary peripheral surface of the worm spiral axis; $X_2Y_2Z_2$ – mobile reference system joined with the in plane wheel of the gear.

The relative position of the global reference systems is defined. The origin of the $x_0y_0z_0$ reference system (the P point) regarding the xyz global reference system is given by vector \vec{a} associated with the matrix, equation (1):

$$a = (r_2 \cos \mu \quad r_2 \sin \mu \quad r_1)^T, \tag{1}$$

where: r_1 is the radius of the reference cylinder of the spiral worm; r_2 is the average radius of the in plane wheel of the hypoid gear; μ is the angular constructive value, specifically for the construction of the spiral gear.

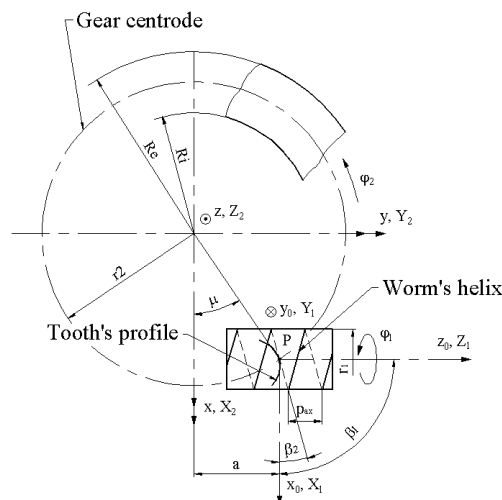


Figure 1. Gearing kinematics.

With φ_1 and φ_2 we denote the angles described, in the same time, in the rotation around its own axis (Z_1 and respectively Z_2) by the spiral worm and by the spiral in plane wheel, respectively.

Obviously, between these two motions, the gear ratio is defined, equation (2):

$$i = \frac{\varphi_1}{\varphi_2} = \frac{z_2}{z_1} = cst, \tag{2}$$

where z_1 is the starts number of the spiral worm and z_2 is the number of teeth of the in plane wheel.

We denote with x and x_0 the coordinate of points in the global reference systems and with X and X_1 the coordinates of points in the mobiles reference systems.

The assembly of the absolute allows determining the relative motion between the mobile reference systems, $X_1Y_1Z_1$ and $X_2Y_2Z_2$, equation (3):

$$X_2 = \omega_3(\varphi_2) \left[\alpha^T \omega_3^T(\varphi_1) X_1 + a \right], \quad \alpha = \begin{pmatrix} 1 & 0 & 0 \\ 0 & 0 & 1 \\ 0 & 1 & 0 \end{pmatrix}. \quad (3)$$

During the movement (2), the surface family generated by the spiral worm flanks is determined in the reference system joined with the in plane wheel of the gear.

Obviously, in equation (2), the X_1 matrix denotes the matrix formed with the coordinates of the current point on the flank of the gear's worm.

The enveloping of the surface family generated by the flanks of the worm in the movement (2) represents the surface of the in plane wheel flanks of the spiral gear.

In principle, the worm flank equations have the following form equation (4):

$$\Sigma | X_1 = X_1(u, \theta); Y_1 = Y_1(u, \theta); Z_1 = Z_1(u, \theta), \quad (4)$$

with u and θ as independent variable parameters.

In this way, from (2), the Σ surface family in the mobile reference system, joined with the in plane wheel, has the equations depend on three parameters, equation (5):

$$(\Sigma)_{X_2Y_2Z_2} : | X_2 = X_2(u, \theta, \varphi_1); Y_2 = Y_2(u, \theta, \varphi_1); Z_2 = Z_2(u, \theta, \varphi_1). \quad (5)$$

The enveloping of the surface family (4), obtained through the association between the family equations and the specifically enveloping condition, represent the flank of the in plane teathed wheel, conjugated with the helicoidally worm.

3. Enveloping condition

The enveloping condition in the Gohman form, as is presented by Litvin et al [4] and also by Radzevich [6], equation (6):

$$\vec{N}_\Sigma \cdot \vec{R}_\varphi = 0 \quad (6)$$

written in the $X_1Y_1Z_1$ reference system, assuming that the two vectors are defined in the same reference system. In principle, the directrix parameters of the normal to Σ are possible to be defined from equation (4), in the $X_1Y_1Z_1$ reference system, equation (7)

$$\vec{N}_\Sigma = \begin{vmatrix} \vec{i} & \vec{j} & \vec{k} \\ \dot{X}_{1u} & \dot{Y}_{1u} & \dot{Z}_{1u} \\ \dot{X}_{1\theta} & \dot{Y}_{1\theta} & \dot{Z}_{1\theta} \end{vmatrix} = N_{X_1} \vec{i} + N_{Y_1} \vec{j} + N_{Z_1} \vec{k} \quad (7)$$

with $\dot{X}_{1u}, \dot{Y}_{1u}, \dot{Z}_{1u}$ and $\dot{X}_{1\theta}, \dot{Y}_{1\theta}, \dot{Z}_{1\theta}$ as partial derivatives of equation (4) regarding the variables u and θ , respectively.

The vector is the velocity vector in the relative motion of the $X_2Y_2Z_2$ reference system, joined with the in plane teathed wheel, regarding the worm reference system.

It is defined from (3), equation (8):

$$X_1 = \omega_3(\varphi_1) \alpha \left[\omega_3^T(\varphi_2) X_2 - a \right] \quad (8)$$

the relative motion of the points of the $X_2Y_2Z_2$ reference system regarding the $X_1Y_1Z_1$ reference system. Starting from equation (7), equation (9):

$$R_{\varphi_1} = \frac{dX_1}{d\varphi_1} = \dot{\omega}(\varphi_1)\alpha[\omega_3^T(\varphi_2)X_2 - a] + \omega_3(\varphi_1)\alpha\dot{\omega}_3^T(\varphi_2)\frac{d\varphi_2}{d\varphi_1}X_2, \tag{9}$$

the velocity vector (with the same direction) in the relative motion of the in plane wheel regarding the helical worm is defined. With the gear ratio was denoted (see equation (2)).

After replacements and developing, the (8) equation may be brought to form (see figure 1):

$$R_{\varphi_1} = \begin{pmatrix} Y_1 - iZ_1 \cos \varphi_1 + r_2 \sin(\varphi_1 - \mu) - r_1 i \cos \varphi_1 \\ -X_1 + iZ_1 \sin \varphi_1 + r_2 \cos(\varphi_1 - \mu) - r_1 i \sin \varphi_1 \\ X_1 \cos \varphi_1 - Y_1 \sin \varphi_1 \end{pmatrix}. \tag{10}$$

In principle, the enveloping condition (5), regarding (6) and (8), is a function in form of equation (11):

$$Q(u, \theta, \varphi_1) = 0 \tag{11}$$

with u, θ and φ_1 as variable parameters.

The family of surfaces of the helical worm's flanks in the in plane wheel is obtained from (2), in principle, equation (12):

$$(\Sigma)_{\varphi_1} | X_2 = X_2(u, \theta, \varphi_1); Y_2 = Y_2(u, \theta, \varphi_1); Z_2 = Z_2(u, \theta, \varphi_1). \tag{12}$$

The assembly of equations (9), (11) and the condition:

$$\varphi_1 = const. \text{ (usually, } \varphi_1 = 0 \text{)}, \tag{13}$$

represent, in principle, the common characteristic curve of the helical surface and the flank of the in plane wheel.

4. Helical worm with straight line profile

Now, it is possible to write the enveloping condition specific for each flank (see form (5)) and the expression of the velocity vector (8).

If the enveloping conditions are known, it is possible to determine, in numerical form, the characteristic curves.

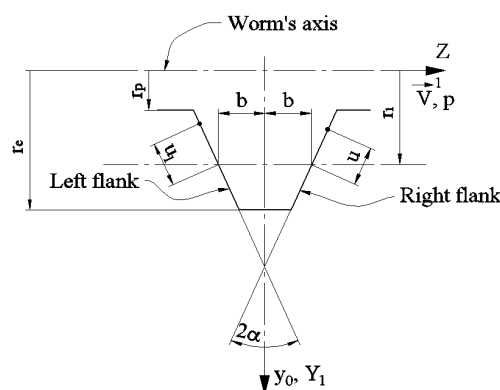


Figure 2. Axial section of Archimedes's worm.

For the case: $i=z_1/z_2=60/1$; $r_f=15.03$ mm; $r_e=37.2$ mm; $p=9.42$ mm; $\alpha=20^\circ$, the contact lines T_{right} and T_{left} are calculated, defining also their length along the flank.

The contact line represents the curves along which the helical surfaces are tangents in relation with the flank surfaces of the in plane toothed wheel.

The modification of the worm geometry is proposed in order to improve the function of this gear type.

5. Helical worm with circular profile

An axial profile of the worm is proposed, as presented in figure 3.

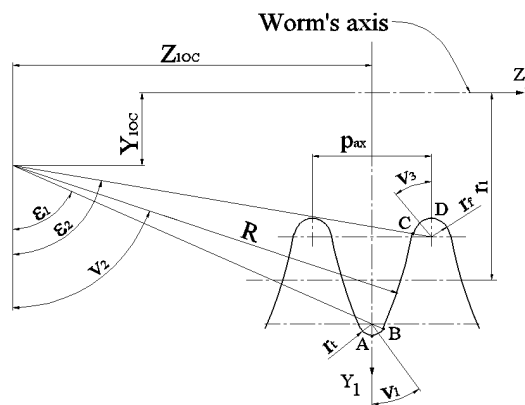


Figure 3. Axial section of the worm with circular profile.

Similarly, it is possible to define a variant of spiral worm with an axial profile composed by an assembly of circle arcs and a convex profile, with equations given in table 1.

Table 1. Parametrical equations of the axial generatrix of the spiral worm with curved profile.

Arc	Variables	Limits
$X_1 = 0 ;$ $AB \quad Y_1 = Y_{1OC} + (R - r_t) \cos \varepsilon_1 + r_t \cos v_1 ;$ $Z_1 = \pm [Z_{1OC} + (R - r_t) \sin \varepsilon_1 + r_t \sin v_1] .$	v_1	$v_{1min} = 0 ;$ $v_{1max} = \varepsilon_1 .$
$X_1 = 0 ;$ $BC \quad Y_1 = Y_{OC} + R \cos v_2 ;$ $Z_1 = \pm (Z_{1OC} + R \sin v_2) .$	v_2	$v_{2min} = \varepsilon_1 ;$ $v_{2max} = \varepsilon_2 .$
$X_1 = 0 ;$ $CD \quad Y_1 = Y_{1OC} + (R + r_f) \cos \varepsilon_2 - r_f \cos v_3 ;$ $Z_1 = \pm [Z_{1OC} + (R + r_f) \sin \varepsilon_2 - r_f \sin v_3] .$	v_3	$v_{3min} = 0 ;$ $v_{3max} = \varepsilon_2 .$

Note: p_{ax} is the axial pitch of the worm, $p_{ax}=9.42$ mm; r_t is the top radius of the profile, $r_t=1$ mm; p – helical parameter, $p = p_{ax}/2\pi$; the lower sign for Z_1 is for the left flank.

The surface of the spiral worm helical flank is obtained in the generatrix helical movement, equation (14):

$$\begin{pmatrix} X_1 \\ Y_1 \\ Z_1 \end{pmatrix} = \begin{pmatrix} \cos \theta & -\sin \theta & 0 \\ \sin \theta & \cos \theta & 0 \\ 0 & 0 & 1 \end{pmatrix} \cdot \begin{pmatrix} X_1(v_i) \\ Y_1(v_i) \\ Z_1(v_i) \end{pmatrix} + \begin{pmatrix} 0 \\ 0 \\ p \cdot \varphi \end{pmatrix}, \quad (14)$$

with $(i=1, 2, 3)$.

The normal to the helical flank with vectors on type, equation (15):

$$\vec{N}_\Sigma = \begin{vmatrix} \vec{i} & \vec{j} & \vec{k} \\ \dot{X}_{1v_i} & \dot{Y}_{1v_i} & \dot{Z}_{1v_i} \\ \dot{X}_{1\theta} & \dot{Y}_{1\theta} & \dot{Z}_{1\theta} \end{vmatrix} \quad (15)$$

is calculated for $i=1, 2, 3$ – and the equations in table 1 and $\dot{X}_{1v_i}, \dot{Y}_{1v_i}, \dot{Z}_{1v_i}, \dot{X}_{1\theta}, \dot{Y}_{1\theta}, \dot{Z}_{1\theta}$, partial derivative of the flank's equations (see table 1).

The velocity vector, \vec{R}_{φ_1} , has the form (9) for X_1, Y_1 and Z_1 in table 1.

For $\varphi_1=\text{constant}$ ($\dot{\varphi}_1=0$) the assembly equations determined by the family (11), with the specifications in table 1 and the enveloping condition (5), with the specifications (9), (14) and table 1 determine the new form of the characteristic curve, for the modified worm.

6. Numerical results

In house software in Matlab program was made for the calculus of the new contact line (the characteristic curve) for the two situations.

The ruler worm has the following characteristic (see figure 1):

$z_1=1$, the number of worm beginnings;

$z_2=60$, the number of teeth for in plane wheel;

$m_n=3$ mm, the worm normal module;

$r_1=15.03$ mm, the worm average radius;

$\mu=45^\circ$;

$r_2=100$ mm, the average radius of the in plane wheel;

$\beta_2=44.09^\circ$ is the angle of the in plane wheel teeth (see figure 1);

$a=64.642$ mm is the distance between the worm axis and the in plane wheel;

$p_{ax}=9.42$ mm, axial pitch of the spiral worm.

For the normal modulus, equation (16):

$$m_n = \frac{2r_2 \cos \beta_2}{z_2}, \quad (16)$$

the reference radius of the toothed wheel is calculated (see figure 2), equation (17):

$$r_1 = \frac{z_1 m_n}{2 \cos \beta_1}. \quad (17)$$

The μ angle is defined (see figure 1), equation (18):

$$\mu = \beta_1 - \beta_2; \quad \sin \mu = \frac{a}{r_2}; \quad \beta_2 = 44.09^\circ; \quad \beta_1 = 89.09^\circ; \quad (18)$$

- the worm axial apparent pitch, for a worm with z_1 beginnings, equation (19)

$$p_{ax} = \frac{2\pi r_1}{z_1 \tan \beta_1} \quad (19)$$

The software allows for numerical applications for the determination of the contact line form between the spiral worm and the in plane wheel.

In the same time, the software allows for the 3D representation of the in plane wheel model and the determination of the contact curve length.

Figure 4 presents the form and coordinates of the characteristic curve in the reference system joined with the spiral worm. In the following, this characteristic curve is transposed in the reference system of the wheel in order to determine the characteristic curve of the gear. In this way, the shape of primary peripheral surface is determined.

The length of the contact line between the flank of the spiral worm and the in plane wheel is $L=7.715$ mm.

The dimensions of the worm are: $r_f=15.03$ mm; $r_2=100$ mm; $\alpha=20^\circ$; $p_{ax}=9.42$ mm (worm pitch); number of worm starts $z_1=1$; number of wheel teeth $z_2=60$.

Similarly, with the previous algorithm, the contact line is calculated for a worm with circular generatrix (see figure 3).

The form of the contact line is defined between the flank of the spiral worm and the flanks of the in plane toothed wheel, by the same method, as presented previously.

For a gear with dimensions:

$r_f=1$ mm; $z_1=1$; $r_f=15.03$ mm; $r_2=100$ mm; $R=31.1$ mm;

$r_f=1.5$ mm; $z_2=60$; $\varepsilon_1=65.94^\circ$; $\varepsilon_2=80.24^\circ$; $p_{ax}=9.42$ mm;

$Y_{IOC}=5.84$ mm; $Z_{IOC}=\pm 28.40$ mm (for left or right flank).

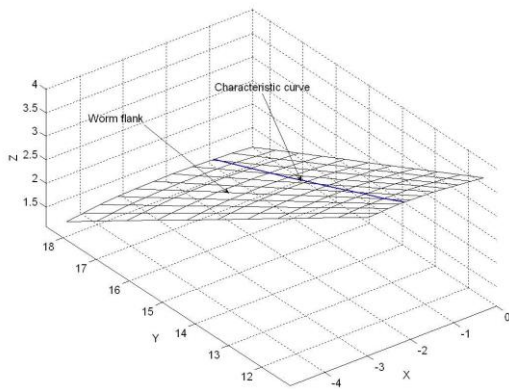


Figure 4. Characteristic curve onto the worm flank (length of contact line $L=7.715$ mm).

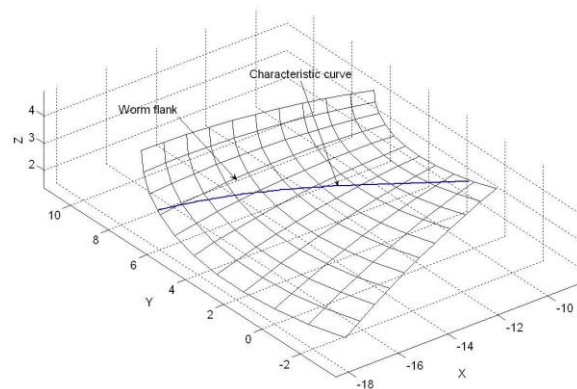


Figure 5. Characteristic curve onto the worm circular arc flank (length of contact line $L=11.186$ mm).

7. Hob mill design element

The machining of the new type of worm for the spiral gear assumes the machining of a new type of tool for the generation of the in plane wheel of the gear.

The hob mill made based on a primary worm identical with the spiral worm will be calculated regarding the constructive elements of the cylindrical worm with circular axial profile.

The geometrical elements of the hob mill are presented in figure 6.

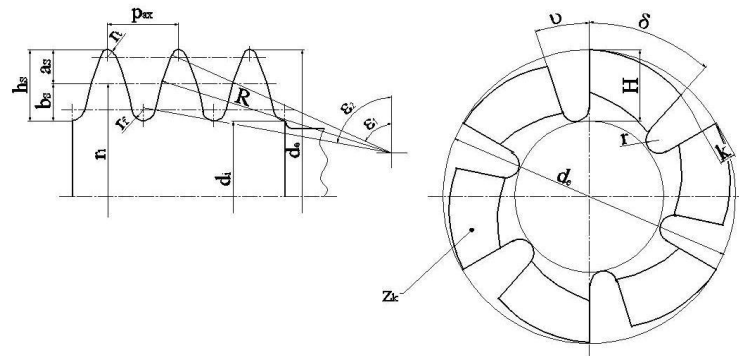


Figure 6. Geometrical elements of the spiral hob mill.

The reference radius, $r_l=15.03$ mm;

The addendum, $a_s=4.49$ mm;

The dedendum, $b_s=4.99$ mm;

The overall height of the gear tooth, $h_s=9.48$ mm;

The addendum diameter, $d_e=39.04$ mm;

The dedendum diameter, $d_i=20.08$ mm;

The starts number of the hob mill, $z_s=1$;

The number of teeth, $z_k=6$ teeth; the number of teeth is chosen from a constructive point of view and it is recommendable

- not to be divisible with the number of starts of the mill and not to be divisor of the number of teeth of the wheel;

- to be an even number in order to ease the control and construction;

- in case of radial feed teething, to be as big as possible to improve the quality of machining.

The relieving, $k=2.5$ mm;

The flute for chip evacuation, $H=13$ mm;

Fillet radius at the flute bottom, $r=1.87$ mm;

The profile angle of the flutes, $\nu=18^\circ$.

8. Conclusions

The issue of the analysis of the worm spiral gear is based onto the principles of the surfaces enveloping with linear contact — the first theorem of Olivier.

The algorithm presented and the software dedicated allow for the determination of the tooth form for the in plane wheel and the length of the contact line between the flanks of the worm and of the wheel.

A new form of the worm for the spiral gear was proposed, characterized by the fact that it does not lead to the formation of crossing curves onto the profile of the in plane wheel and, in the same time, ensures a longer contact line with positive repercussions regarding the gearing function (the decreasing of the load of the wheel flank or the increasing of the transmitted torque).

The number of teeth is chosen from a constructive point of view and it is recommendable: not to be divisible with the number of starts of the mill and not to be divisor of the number of teeth of the wheel; to be an even number in order to ease the control and construction and in case of radial feed teething, to be as big as possible to improve the quality of machining.

The experimental study of the torque of the reducer allows for the highlighting of the resistant torque, for various input speed of the worm and hence the increase of the yield.

We consider that the errors of the worm and the wheel, due of the machining technology, have significant influence on the yield of the reducer.

9. References

- [1] Boloş V and Boloş C 2007 The Mathematical and Numerical Model of the Spiroid Gear with Reverse Tapered *Interdisciplinary in engineering scientific international conference*, Tg. Mureş, Romania p I-45-1-I-45-4
- [2] Boloş V 2010 Achievements of Study Concerning Worm Face Gear Made in Romania *Scientific Bulletin of the "Petru Maior" University of Tîrgu Mureş* **7**(2) (XXIV) 37-40
- [3] Frumuşanu G and Oancea N 2012 Technological solution to profile and generate the teeth of central gear for precessional gear drives *International Journal of Advanced Manufacturing Technology* DOI: 10.1007/S00170-012-4515-3 (Springerlink)
- [4] Litvin F L, Egelja A M and De Donno M 1998 Computerized Determination of Singularities and Envelopes to Families of Contact Lines on Gear Tooth Surfaces *Computer Methods Applied Mechanics and Engineering* **158**(1-2) 23-34
- [5] Kolivand M and Kahraman A 2009 A load distribution model for hypoid gears using ease off topography and shell theory *Mechanism and Machine Theory* (Elsevier) **44** 1848-1865
- [6] Radzevich S P 2008 Kinematic Geometry of Surface Machining *Taylor & Francis Group* ISBN 978 1 4200 6340 0
- [7] Riliang L, Xianzhi Z, Chengrui Z and Lu W 2008 A Design-By-Feature Approach to Step-Compliant NC Programming *International Journal of Innovative Computing, Information and Control* **4**(3) 639-649
- [8] Stanieck R 2011 Shaping of Face Tothing in Flat Spiroid Gears *Journal of Mechanical Engineering* **57** 47-54
- [9] Vogel O, Griewank A and Bar G 2002 Direct gear tooth contact analysis for hypoid bevel gears *Computer Methods in Applied Mechanics and Engineering* **191**(36) 3965-3982